J. Mol. Biol. (1990) **216**, 1017–1029

X-ray Analyses of Aspartic Proteinases

III†. Three-dimensional Structure of Endothiapepsin Complexed with a Transition-state Isostere Inhibitor of Renin at 1·6 Å Resolution

B. Veerapandian, J. B. Cooper, A. Šali and T. L. Blundell‡

Laboratory of Molecular Biology
Department of Crystallography, Birkbeck College
Malet Street, London WC1E 7HX, U.K.

(Received 17 April 1990; accepted 31 July 1990)

The aspartic proteinase, endothiapepsin (EC 3.4.23.6), was complexed with a highly potent renin inhibitor, H-261 (*t*-Boc-His-Pro-Phe-His-Leu$\underline{^{OH}}$Val-Ile-His), where $\underline{^{OH}}$ denotes a hydroxyethylene (-(S)CHOH-CH_2-) transition-state isostere in the scissile bond surrogate. Crystals were grown in a form that has the same space group $P2_1$ as the uncomplexed enzyme, but with a 10 Å decrease in the length of the *a*-axis and a 13° decrease in the β-angle. X-ray data have been collected to a resolution of 1·6 Å. The rotation and translation parameters defining the position of the enzyme in the unit cell were determined previously using another enzyme–inhibitor complex that crystallized isomorphously with that of H-261. The molecule was refined using restrained least-squares refinement and the positions of non-hydrogen atoms of the inhibitor and water molecules were defined by difference Fourier techniques. The enzyme–inhibitor complex and 322 water molecules were further refined to a crystallographic *R*-factor of 0·14. Apart from a small rigid group rotation of a domain comprising residues 190 to 302 and small movements in the flap, there is little difference in conformation between the complexed and uncomplexed forms of the enzyme. The inhibitor is bound in an extended conformation along the active site cleft, and the hydroxyl group of the hydroxyethylene moiety is hydrogen-bonded to both catalytic aspartate carboxylates. The complex is stabilized by hydrogen bonds between the main-chain of the inhibitor and the enzyme. All side-chains of the inhibitor are in van der Waals' contact with groups in the enzyme and define a series of specificity pockets along the active site cleft. The study provides useful clues as to how this potent renin inhibitor (IC_{50} value of $0{\cdot}7 \times 10^{-9}$ M) may bind renin. In particular it defines the interactions of the hydroxyethylene transition-state isostere with the enzyme more precisely than has been previously possible and therefore provides a useful insight into interactions in the transition state complex.

1. Introduction

Aspartic proteinases are associated with the onset of several pathological conditions such as hypertension (renin), gastric ulcers (pepsin), muscular dystrophy and neoplastic diseases (cathepsins D and E), so their inhibition is of considerable clinical interest. The recent discovery that the retroviral proteinases are also related to the pepsin-like aspartic proteinases has stimulated further interest, especially in view of the possibility that their inhibition could retard viral replication.

The plasma enzyme renin catalyses the rate-limiting cleavage of angiotensinogen to yield the decapeptide angiotensin-I (AI§). Subsequent removal of the carboxy-terminal dipeptide from AI is carried out by angiotensin converting enzyme (ACE) thereby yielding angiotensin II (AII). Binding of AII to its receptor initiates vasco-

† Paper II in this series is Cooper *et al.* (1990).

‡ Author to whom all correspondence should be addressed.

§ Abbreviations used: AI, angiotensin-I; ACE, angiotensin converting enzyme; AII, angiotensin II; HIV-1, human immunodeficiency virus; r.m.s., root-mean-square.

0022–2836/90/241017–13 $03.00/0

constriction and retention of sodium and water in the kidneys. This in turn increases the blood volume and consequently increases the blood pressure. ACE is the target for a number of drugs such as Captopril and Enalopril, which are commercially available and used in the treatment of hypertension, hyperaldosteronism and congestive heart failure (Ondetti & Cushman, 1980). However, renin inhibitors may have some advantages in the control of hypertension as they can be very specific.

Progress in the development of renin inhibitors has centred around the design and analysis of the analogues of the minimal substrate sequence, residues 6 to 13 of angiotensinogen. Inhibitors, in which the Leu–Val scissile bond in the octapeptide sequence of human angiotensinogen is replaced by various non-hydrolysable analogues e.g. $-CH_2-NH-$, lower blood pressure both in primates (Tree *et al.*, 1983) and humans (Webb *et al.*, 1985).

Pepstatin, which has a K_i value of 5×10^{-11} M for pepsin (Workman & Burkitt, 1979), requires a central statine for potent inhibition (Rich *et al.*, 1980; Rich & Bernatowicz, 1982). The main-chain $-CHOH-CH_2-CO-NH-$ ((S)-enantiomer) group was later shown by X-ray analysis to bind the catalytic aspartate groups of the enzyme (James *et al.*, 1982; Bott *et al.*, 1982), the hydroxyl forming hydrogen bonds to both enzyme carboxyl groups. Thus, inhibitors with statine as the central residue in sequences otherwise similar to the angiotensinogen cleavage site proved to be useful inhibitors (Szelke *et al.*, 1982; Boger *et al.*, 1985). Substitution of a shorter hydroxyethylene isostere ($-CHOH-CH_2-$) ((S)-enantiomer) resulted in a very highly potent human renin inhibitor (H-261) with an inhibition constant of 0·7 nM (Szelke *et al.*, 1985). This compound is also a good inhibitor of the HIV-1 proteinase (Richards *et al.*, 1989). In this compound the -CHOH- function is assumed to mimic the tetrahedral geminal diol and the $-CH_2-$ function mimics the $-NH_2^+$ of the transition state. X-ray structural studies of different analogues complexed with endothiapepsin are reviewed by Cooper & Harris (1989) and Blundell *et al.* (1987).

X-ray studies of the potent hydroxyethylene inhibitor of human renin, H-261, complexed with endothiapepsin were initially carried out on crystals that were isomorphous with those of the native enzyme, but data were collected only to medium resolution (Blundell *et al.*, 1987). More recently we found that under the same conditions a less disordered crystal form that contains less solvent and diffracts to higher resolution (1·6 Å, 1 Å = 0·1 nm) could be obtained over a longer crystallization period. Here, we report details of the three-dimensional structure of the complex with emphasis on the description of enzyme–inhibitor interactions and on the nature of the specificity sub-sites. Since we have been able to collect data from these crystals to a higher resolution than for any other inhibitor, the analysis of the three-dimensional structure is the most accurate of the endothiapepsin complexes. Thus, the enzyme structure is also briefly described and compared to that of the native structure (Blundell *et al.*, 1985, 1990; paper I in this series).

2. Experimental

(a) *Synthesis of inhibitor*

The inhibitor, H-261, has a formula *t*-Boc-His-Pro-Phe-His-Leu$\underline{^{OH}}$Val-Ile-His, where *t*-Boc is tertiary butoxycarbonyl and $\underline{^{OH}}$ denotes a hydroxyethylene ($-CHOH-CH_2-$) transition-state isostere in the scissile bond surrogate. All chiral centres, including those of the isostere, are of the S-form. The inhibitor was synthesized using the procedures described by Szelke *et al.* (1985) and provided by Dr M. Szelke as freeze-dried samples, which had a quoted purity of about 90%.

(b) *Crystallization*

Endothiapepsin was extracted from a fungal rennet, Sure-curd, from Pfizer Inc., by successive ammonium sulphate precipitations (Whitaker, 1970). Crystals of endothiapepsin complexed with the synthetic inhibitor were grown by an adaptation of the method described by Moews & Bunn (1970), which involves a protein concentration of 2 mg/ml in 0·1 M-sodium acetate buffer (pH 4·6). A sufficient quantity of the inhibitor was added to a weighed sample of the enzyme to give a 10-fold molar excess of the inhibitor. To ensure complex formation they were stirred together in the crystallization buffer for several hours before filtration and addition of the fine ground ammonium sulphate to 55% saturation (2·2 M). The solution was filtered into 2 ml batches and a few drops of acetone were added to each. These were left to crystallize at room temperature for several months after which good crystals appeared.

The crystal data for the enzyme–inhibitor complex are given in Table 1. The crystals are non-isomorphous with

Table 1

Crystal data and a summary of refinement statistics

Space group	$P2_1$
Unit cell dimensions	$a = 43{\cdot}0$ Å
	$b = 75{\cdot}7$ Å
	$c = 42{\cdot}9$ Å
	$\beta = 97{\cdot}1°$
Number of molecules per unit cell	2
Relative molecular mass of protein	$M_r = 33{,}903$
Number of residues in protein molecule	330
Number of protein atoms	2389
Number of inhibitor atoms	79
Number of solvent atoms located	322
Number of sulphate ions	3
Number of symmetry-independent reflections	31,666
Number of reflections with $I \geq 2\sigma(I)$	28,014
R-merge	5·5%
r.m.s. deviation from target bond lengths	0·024 Å
r.m.s. deviation from target angle distances	0·045 Å
r.m.s. deviation from peptide planarity	0·008 Å
r.m.s. deviation from side-chain planarity	0·006 Å
Average B_{iso} for protein atoms	10·6 Å^2
Average B_{iso} for main-chain atoms	8·4 Å^2
Average B_{iso} for inhibitor atoms	18·3 Å^2
Average B_{iso} for solvent atoms	35·2 Å^2
Average B_{iso} for all atoms	13·8 Å^2
Final *R*-factor ($\Sigma\|\|F_{obs}\|-\|F_{calc}\|\|/\Sigma\|F_{obs}\|$)	0·1419
r.m.s. shift in co-ordinates in final cycle	0·008 Å

the original form obtained from the uncomplexed enzyme and for some inhibitor complexes (Foundling *et al.*, 1987; Blundell *et al.*, 1987, and references cited therein). Although the space group remains $P2_1$, as for the uncomplexed endothiapepsin, the unit cell dimension along the a-axis is shorter by about 10 Å and the β-angle is 13° smaller. Crystals isomorphous to the H-261 complex had previously been obtained for a complex of endothiapepsin with another inhibitor (BW625), which was solved by molecular replacement (Cooper, 1989). This crystal form has closer packing in the unit cell giving an estimated solvent content of 39% as compared with 55% for the native crystal form. The new crystals diffract to a higher resolution than native crystals allowing collection of X-ray data to 1·6 Å resolution.

(c) *Data collection and structure determination*

Four crystals were employed in collecting the diffraction data to a resolution of 1·6 Å using an Enraf-Nonius CAD4 diffractometer. A total of 38,375 reflections were recorded and collected for radiation decay, Lorentz-polarization and absorption (North *et al.*, 1968). The F_{obs} values were merged (Rae, 1965; Rae & Blake, 1966) to give a unique set of 31,666 reflections with a merging R-factor of 0·055. The endothiapepsin co-ordinates obtained in the analysis of the complex with BW625 (Cooper, 1989) were used to calculate the structure factor amplitudes F_{calc} and phases (α_{calc}). These were scaled to the observed amplitudes, F_{obs}, using the program SIMWT (Tickle, 1988). Difference Fourier maps with coefficients $F_{obs}-F_{calc}$ and $2F_{obs}-F_{calc}$ were computed using the α_{calc} values and displayed on an Evans and Sutherland PS300 graphics system using FRODO (Jones, 1978). Clear and contiguous electron density for the inhibitor made modelling straightforward with the exception of the C-terminal residue where the density is weak. The same is found for many inhibitors complexed with endothiapepsin.

The resulting model of the enzyme complex was then subjected to stereochemically restrained least-squares refinement using the program RESTRAIN (Moss & Morffew, 1982; Haneef *et al.*, 1985). Several cycles of rigid body refinement placed the molecules more precisely in the unit cell. Subsequently all atomic co-ordinates and isotropic temperature factors were refined by gradual inclusion of the high resolution reflections, initially to 1·8 Å and later to 1·6 Å. During the course of refinement the model was inspected by computing difference Fourier maps with coefficients $2F_{obs}-F_{calc}$ and $F_{obs}-F_{calc}$. Conformations of the side-chains of some serine, threonine, lysine and other surface residues were remodelled and water molecules were gradually included to give a total of 322 in the final cycles of refinement. A comparison of the isotropic temperature factors of the inhibitor and those of the enzyme indicated that the inhibitor is present at unit occupancy. The refinement was concluded after 125 cycles of least-squares optimization when the final cycle had an r.m.s. shift in atomic co-ordinates of 0·008 Å.

The least-squares fitting programs XS1 and XS2, written by A. Šali applying the method described by McLachlan (1982), were used for pairwise superposition of molecules.

3. Results and Discussion

(a) *The quality of the analysis*

The final refined model of the complex had 2389 enzyme atoms, 79 inhibitor atoms, 3 sulphate ions and 322 solvent molecules. The final R-factor was 0·14 for 28,014 reflections in the 20 Å to 1·6 Å resolution range with $F_{obs} \geq 2\sigma(F_{obs})$. A summary of the refinement statistics is given in Table 1. The parameters for bond lengths and angles are well within the range of known small molecules. The error in the atomic co-ordinates was estimated by the method described by Luzzati (1952) to be 0·10 Å (Fig. 1).

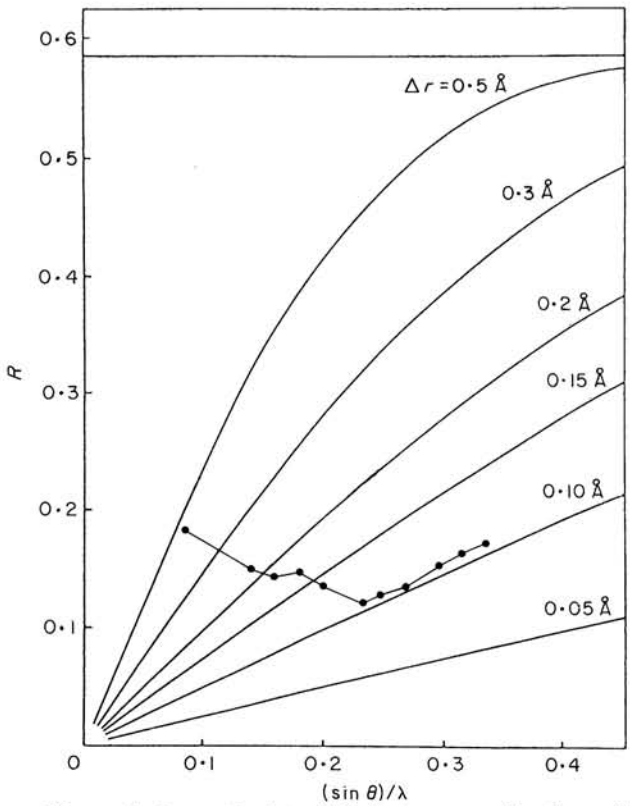

Figure 1. Luzzati plot of R-factor as a function of $(\sin\theta)/\lambda$. The error in the co-ordinates (Δr) is about 0·10 Å.

Almost all of the atoms in the inhibitor could be identified from the electron density maps. Figure 2

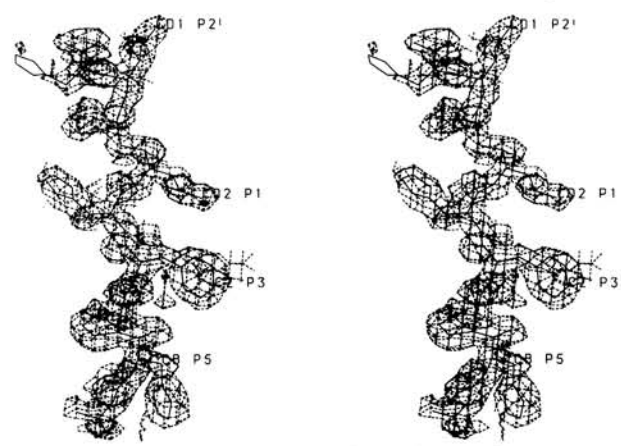

Figure 2. Stereo view of the final electron density map calculated using the $2F_{obs}-F_{calc}$ coefficients for the H-261 inhibitor in the active site of endothiapepsin. The inhibitor side-chains are well defined in all the positions, with the exception of the side-chain of the P'_3 His.

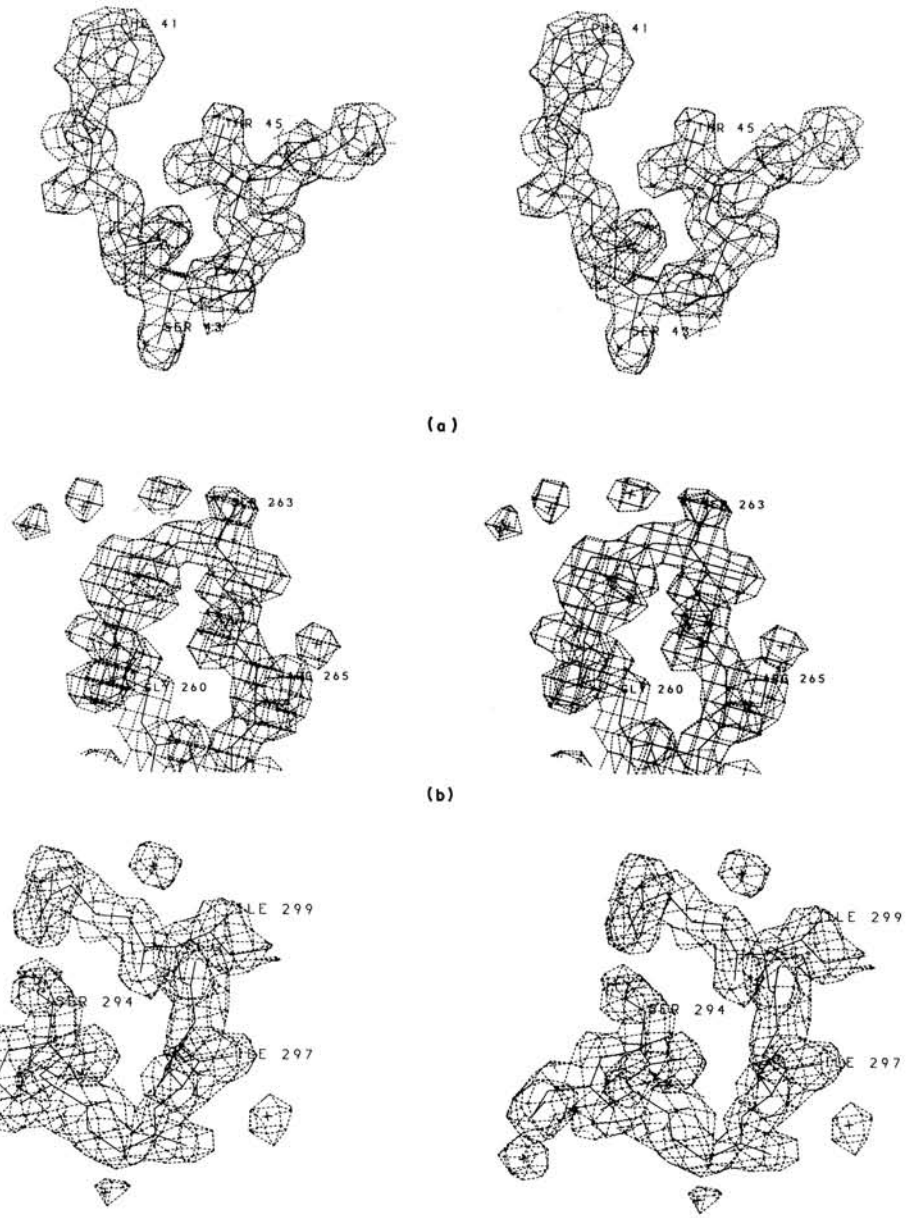

Figure 3. Stereo views of the electron density of 3 surface loops of the enzyme which are disordered in the native structure. (a) Residues 41 to 45; (b) residues 261 to 265 and (c) residues 294 to 298.

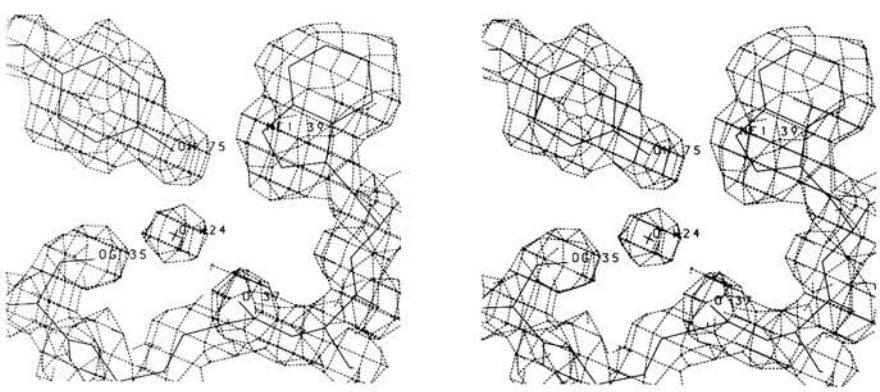

Figure 4. Stereo view of the electron density of Tyr75 and its environment.

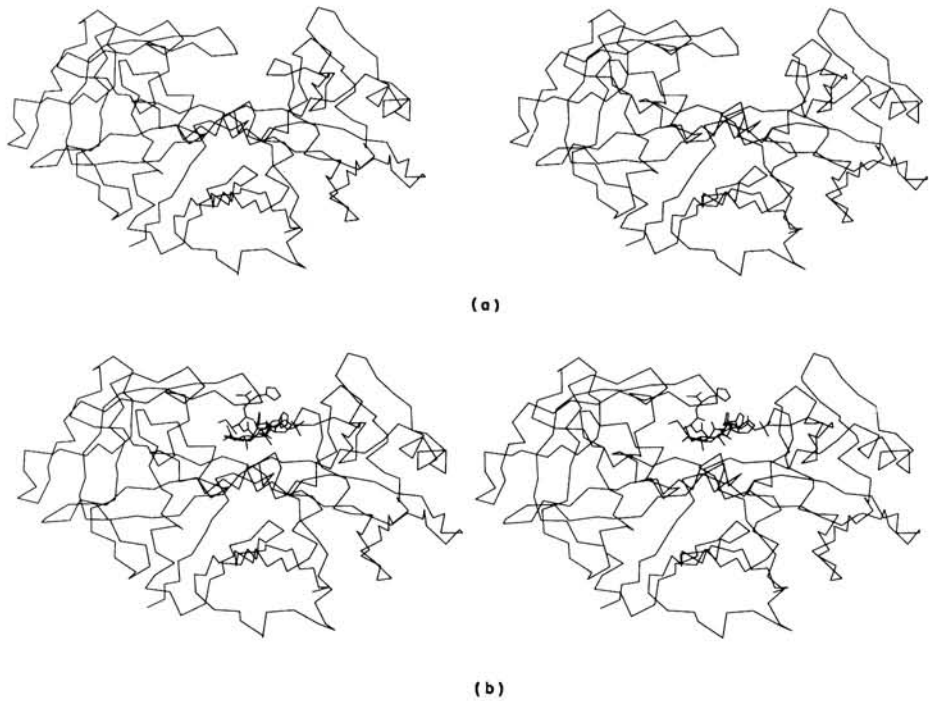

Figure 5. Stereo views of (a) the endothiapepsin molecule (C^{α} atoms only) and (b) its complex with the inhibitor.

is a stereo view of the $2F_{obs}-F_{calc}$ electron density of the inhibitor demonstrating the high quality and clarity of the map. The improved resolution of the data allowed better definition of some regions of the enzyme that are poorly defined in the native crystal structure, especially surface loops (see Fig. 3). The active site "flap" and the solvent molecules with which it interacts are more clearly defined than in the uncomplexed enzyme (Fig. 4). Elsewhere, nine of 11 lysine residues and the lone arginine have their side-chains well defined. Most of the aromatic rings have well-defined planes with central holes.

(b) *The general structure of the enzyme inhibitor complex*

The overall structure of the enzyme molecule is similar to that described earlier (Blundell *et al.*, 1985, 1990). Figure 5 shows stereo views of the enzyme and of its complex with the inhibitor. The active site cleft is formed between the two lobes, each of which provides one of the essential aspartate residues. The inhibitor H-261 has an extended β-strand conformation (Fig. 6) and makes hydrogen bonds throughout its main-chain to each lobe of the enzyme (Fig. 7). The side-chains make hydrogen bonds and van der Waals' interactions with both domains in the molecule so defining sub-sites S_6, S_5, S_4, S_3, S_2, S_1, S'_1, S'_2 and S'_3 (Berger & Schechter, 1970). An antiparallel β-hairpin comprising residues 71 to 82, known as the flap, interacts with the central region of the inhibitor and shields the active site from the solvent. The carboxylate groups of the active site aspartate residues form hydrogen bonds with the hydroxyl oxygen of the hydroxyethylene isostere of the inhibitor (Fig. 8). Although the carboxylates are coplanar in the uncomplexed enzyme, their planes are inclined to each other by about 30° in the complex due to steric interactions with the inhibitor. The carboxy-terminal His at P'_3 loops out into the solvent region.

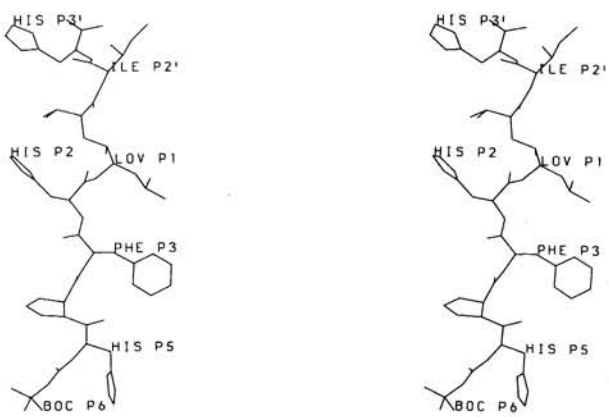

Figure 6. Stereo view of the isolated inhibitor in the bound conformation. The Leu$^{\underline{OH}}$Val residue at P_1–P'_1 is labelled LOV.

The conformational angles of the inhibitor H-261 are given in Table 2. The main-chain ϕ and ψ values of the inhibitor are in the β-sheet area of the Ramachandran plot (Fig. 9). Side-chain conformational angles of the inhibitor are in the range of commonly observed values, as shown in Table 2 and Figure 9.

(c) *Hydrogen bonds*

The inhibitor makes 12 possible hydrogen bonds to the enzyme and six to water molecules (Fig. 7). Nearly every main-chain NH and CO function makes one hydrogen bond, either to the enzyme or

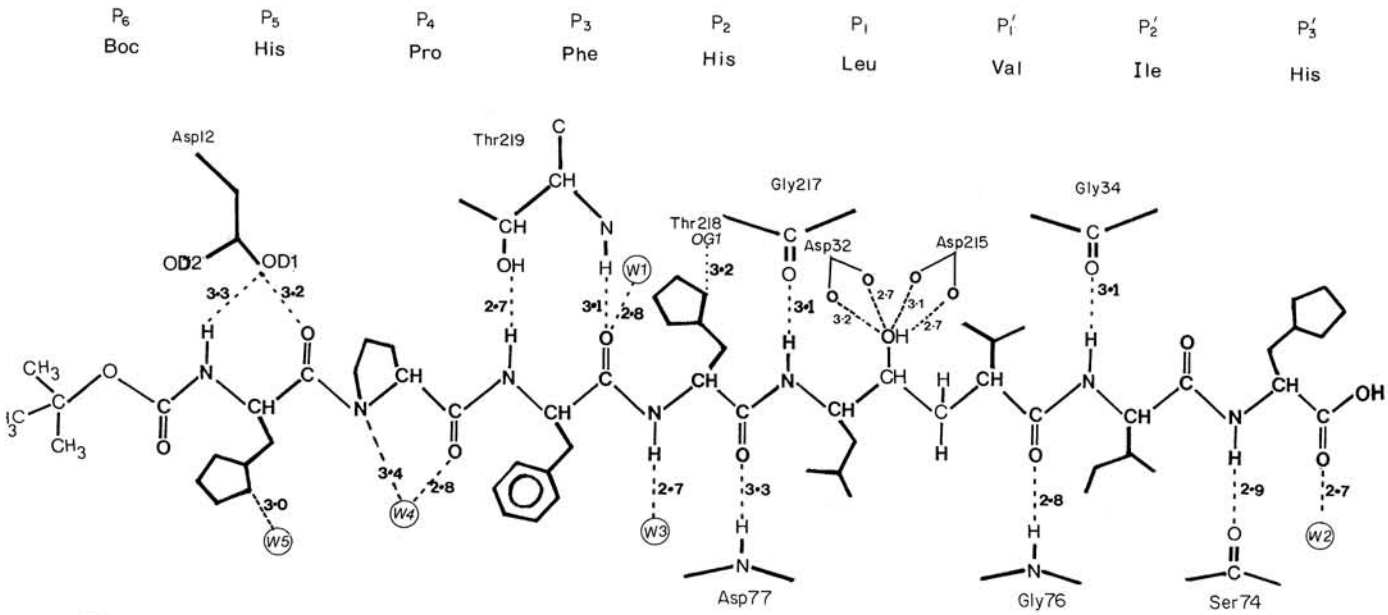

Figure 7. Schematic diagram of possible hydrogen bonds between inhibitor and enzyme. The donor–acceptor distances shorter than 3·4 Å are shown with broken lines.

to water. This gives rise to an antiparallel β-pleated sheet between residues P_3 to P_1 of the inhibitor and one short stretch of residues from the C-terminal lobe of the enzyme, 219 to 217. An equivalent β-sheet interaction with the N-terminal lobe would involve parallel strands if it existed, but only one hydrogen bond of this putative structure is formed involving P'_2 NH and 34 CO. A similar pattern of hydrogen bonds is observed in other inhibitor–aspartic proteinase complexes (Bott *et al.*, 1982; James *et al.*, 1982; Foundling *et al.*, 1987; Blundell *et al.*, 1987; Suguna *et al.*, 1987).

The amide nitrogen of P_5 has a bifurcated hydrogen bond with both the side-chain oxygen atoms of Asp12, one of which also makes a further hydrogen bond with the main-chain CO of P_5. At the S_3 sub-site the amide nitrogen of P_3 makes a hydrogen bond with the side-chain oxygen atom of Thr219, and the main-chain CO forms bifurcated hydrogen bonds with the amide nitrogen of Thr219 and with a water molecule (W1). The main-chain carbonyl oxygen and nitrogen of P_2 are hydrogen-bonded to Asp77 NH and to water (W3), respectively. The P_2 imidazole nitrogen $N^{\delta 1}$ is hydrogen-bonded to the side-chain oxygen of Thr218.

The transition state isostere is held by hydrogen bonds between the -CHOH-CH_2- of the inhibitor and the residues of the conserved Asp-Thr-Gly regions and the flap (see Fig. 8). The hydroxyl group of the hydroxyethylene makes several close contacts with the catalytic aspartate residues and probably forms two hydrogen bonds at the pH of crystallization (pH 4·5). These may involve the side-chain $O^{\delta 1}$ oxygen atoms of Asp32 and Asp215, which show the shortest distances of 2·7 Å. The carboxylate $O^{\delta 2}$ oxygen atoms of the two aspartate residues are at distances of 3·2 and 3·1 Å (Fig. 7). Hence, the inner carboxyl oxygen of Asp32 and the outer oxygen of Asp215 form the closest contacts with inhibitor OH group. The flap is held down by

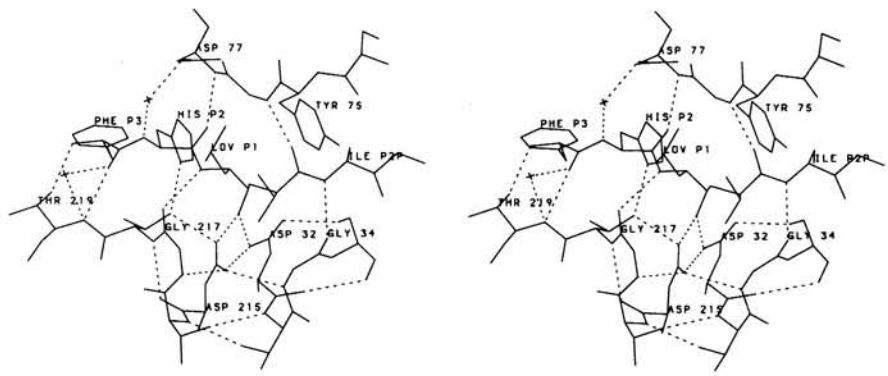

Figure 8. Stereo view of the complex between endothiapepsin and H-261 in the region of P_3–P'_1 showing the hydrogen bond contact distances (broken line) and the extensive van der Waals' contacts between the inhibitor and the enzyme. The stars indicate the positions of the water molecules of ions.

Table 2
Main-chain and side-chain dihedral angles of H-261

Subsite	Residue	Dihedral angles (deg.) ϕ	ψ	ω	χ_1	χ_2
P_5	His	−140	66	−166	−56	−70
P_4	Pro	−79	160	−174	13	−2
P_3	Phe	−108	149	174	−84	−108
P_2	His	−139	88	−170	−178	21
P_1	Leu	−117	54	150	−70	−58
P'_1	Val	−80	148	168	47	
P'_2	Ile	−65	138	175	−176	176
P'_3	His	−116	163		−147	−88

four hydrogen bonds to the inhibitor. The amide nitrogen of Asp77 is hydrogen-bonded to the carbonyl oxygen of P_2 and there exists a weaker hydrogen bond between the same carbonyl oxygen and amide nitrogen of Gly76. The nitrogen of Gly76 is also hydrogen-bonded to the P'_1 carbonyl oxygen and Ser74 CO is hydrogen bonded to the amide nitrogen of P'_3. In addition to these flap interactions the amide nitrogen atoms of P_1 and P'_2 are hydrogen bonded to the carbonyl oxygen atoms of Gly217 and Gly34 as noted above. Thus, the transition state isostere, the active site flap and the catalytic residues are very tightly hydrogen-bonded in an arrangement that provides a geometrically well-defined environment for stabilization of the transition state.

(d) *Water molecules and crystal contacts*

The crystal packing and interactions with water molecules differ from those of the native endothiapepsin crystal form. There are 41 internal water molecules, each defined by four or more hydrogen bonding contacts to the enzyme or to neighbouring water molecules and isotropic temperature factors less than 25 Å^2.

The inhibitor displaces 15 of the 20 water molecules occupying the active site of the uncomplexed enzyme. All polar side-chains of the enzyme that make hydrogen bonds with the inhibitor are also hydrogen-bonded to water molecules in the uncomplexed structure. The water molecule W2, which is bound between the carboxylate groups of the catalytic aspartate residues in the uncomplexed enzyme and may play the role of nucleophile during catalysis (Pearl & Blundell, 1984; Pearl, 1985; Blundell *et al.*, 1987; Suguna *et al.*, 1987), is displaced by the hydroxyl oxygen of the transition-state isostere (Fig. 8). Five of the 17 water molecules that form contacts with the inhibitor are hydrogen-bonded to it, and most are further bridged to the enzyme. The internal water molecule, W1, which is hydrogen-bonded to the inhibitor and to the hydroxyl of Tyr222 also interacts with the loop comprising residues 284 to 294 through a network of water molecules (P_3 O-W1-222 OH-W51-W53-W52-289 OH). W1 also forms hydrogen bonds with the NH

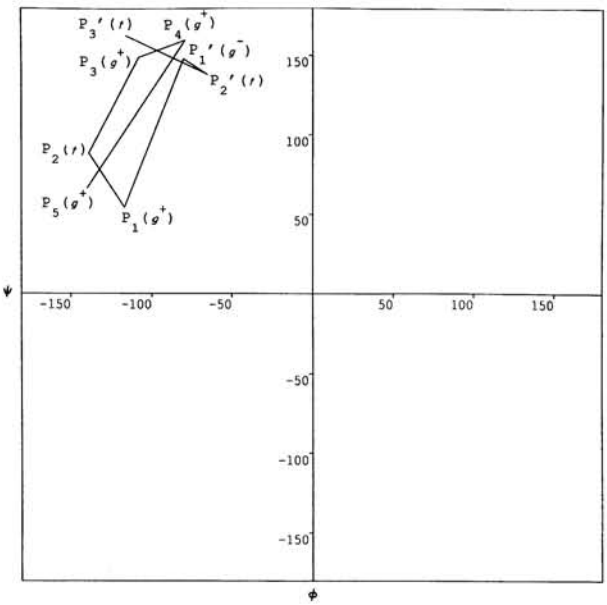

Figure 9. Ramachandran plot giving values of ϕ (horizontal) and ψ (vertical) for the inhibitor. The side-chain conformations are indicated using the nomenclature of Janin *et al.* (1978).

functions of Thr219 and Leu220. Water molecule W3 forms a bridge between the inhibitor and the enzyme (P_2 NH-W3-Asp77 $O^{\delta 1}$), whereas in other complexes such as the reduced bond peptide inhibitor bound to rhizopuspepsin (Suguna *et al.*, 1987), and a pepstatin inhibitor bound to penicillopepsin (James & Sielecki, 1985), the hydrogen bond exists directly between the main-chain nitrogen of P_2 and the oxygen of Asp77 side-chain with no intervening water molecule. In the endothiapepsin–H-261 complex reported here, this water network is extended from Asp77 through W54 to Ser110 O^{γ}. Further water-mediated networks involve P'_3 O-W2-W40-72 O, and P'_3 O-W2-74 N. Such water-mediated hydrogen-bonded bridges may contribute towards the stability of the enzyme–inhibitor complex.

Figure 10 illustrates the crystal packing of the non-isomorphous crystal form adopted by the H-261 complex. Twelve symmetry-related molecules are found to be in contact with the reference molecule, seven of these form 34 possible hydrogen bonds, which are listed in Table 3. In addition, we have interpreted three solvent sites with much more density than usual as sulphate ions. These are on the surface of the molecule and take part in charge-assisted inter-molecular hydrogen bonding. Thus, there is an extensive network of water molecules, ions and inter-molecular interactions that results in the closer packing and lower solvent content of these crystals relative to the native crystal form.

(e) *The specificity sub-sites*

Residues in the specificity sub-sites, S_n were defined as those that have atoms within 4·2 Å of the

Figure 10. The packing of endothiapepsin–inhibitor complexes in the non-isomorphous crystal form viewed down the *c*-axis.

inhibitor residues, P_n (Table 4) and whose area accessible to the solvent is reduced by at least 2 Å^2 (Table 5). The change in solvent accessibility as a function of residue number is given in Figure 11. In the following discussion we do not include main-chain hydrogen bonds; these have been discussed above.

Table 3

Inter-molecular contacts in the crystal with the molecule at X, Y, Z

Residues				Distance (Å)	
$O^{\varepsilon 2}$	Glu49	$O^{\gamma 1}$	Thr318	3·67	(molecule at
$O^{\delta 2}$	Asp51	O	Asp147	2·86	$X, Y, 1+Z$)
N	Gly52	O	Asp147	3·45	
O^{γ}	Ser109	N	Thr318	3·32	
O^{γ}	Ser109	N	Thr319	2·85	
O^{γ}	Ser109	$O^{\gamma 1}$	Thr319	3·92	
$O^{\varepsilon 1}$	Glu113	$O^{\delta 1}$	Asn315	3·87	
$O^{\varepsilon 1}$	Glu113	$N^{\delta 2}$	Asn315	2·84	
O^{γ}	Ser178	O^{γ}	Ser279	3·74	(molecule at
O^{γ}	Ser178	N	Thr280	3·07	$X, Y, Z-1$)
O^{γ}	Ser178	$O^{\gamma 1}$	Thr280	3·46	
$O^{\gamma 1}$	Thr62	O	Ser282	3·79	(molecule at
O	Thr62	N	Gly281	2·83	$1-X, Y+1/2, 1-Z$)
N^{ζ}	Lys64	O	Gly177	2·89	(molecule at $1-X, Y+1/2, -Z$)
$O^{\gamma 1}$	Thr70	N^{ζ}	Lys238A	2·64	(molecule at
O^{γ}	Ser72	O	Gly237	2·62	$-X, Y+1/2, 1-Z$)
O^{γ}	Ser74	O^{γ}	Ser251	3·73	
O^{γ}	Ser80	O^{γ}	Ser236	2·73	
O^{γ}	Ser80	N	Gly237	3·83	
O	Ser80	O^{γ}	Ser236	3·85	
N	Ser81	O	Ser236	3·56	
O^{γ}	Ser81	O	Ser236	2·64	
O^{γ}	Ser81	O	Ala238	3·70	
N^{ζ}	Lys106	O	Trp232	2·95	
N^{ζ}	Lys106	O	Val235	2·86	
N^{ζ}	Lys106	O	Ala238	2·88	
N	Ser108	O^{γ}	Ser236	3·73	
N	Ser126	O	Ser201	3·63	(molecule at
N	Thr127	O	Ser201	3·10	$-X, Y+1/2, -Z$)
N	Thr127	O	Gly202	3·82	
$O^{\gamma 1}$	Thr134	N	Ser204A	3·02	
N	Gln134A	O	Phe203A	3·08	
O^{γ}	Ser282A	O	His P'_3	3·55	(molecule at
O^{γ}	Ser282A	O	His P'_3	3·15	$-X, Y-1/2, 1-Z$

(i) *Sub-site* S_6

The main-chain atoms of the *t*-Boc group (C-O-CO-) and the P_5 (-NH-C^{α}-) are co-planar. This is consistent with several small molecule structures (e.g. see Singh *et al.*, 1987) and is probably due to steric effects of the lone pair orbitals on the alkyl oxygen. van der Waals' interactions are formed between the methyl groups of *t*-Boc and hydrophobic enzyme residues such as Leu10, Phe275 and Phe284, as well as the main-chain carbonyl oxygen atoms of residues 276, 277 and 278 (Table 4). Homology considerations indicate that similar interactions involving Met10 and Tyr275 may exist in complexes with human renin, although residue 284 is a threonine in renin rather than phenylalanine in endothiapepsin.

(ii) *Sub-site* S_5

The S_5 sub-site, a shallow surface region of the N-terminal domain, is more polar than S_6. It contains Asp12, which lies centrally and is responsible for 18 of the 40 van der Waals' contacts and hydrogen bonds with P_5 His. The histidyl side-chain of P_5 is held by a continuous network of hydrogen bonds (P_5 $N^{\delta 1}$-W222-W136-8 $O^{\delta 1}$-12 $O^{\delta 2}$, 12 $O^{\delta 1}$-P_5 N).

(iii) *Sub-site* S_4

This sub-site is continuous with S_5 and S_3, but extends into the C-terminal domain. P_4 Pro makes a few close contacts involving the side-chains of Asp12, Thr219 and Leu220. The conformational parameters P_5 ψ and P_4 ϕ (Table 2) lead to a bend in the generally extended main-chain that matches the active site cleft.

(iv) *Sub-site* S_3

P_3 Phe has more contacts than any other inhibitor residue; it makes van der Waals' interactions with a number of hydrophobic residues, e.g. Ile7, Ala13, Ile117 as well as the polar residues Asp12 and Asp114. The phenyl ring of P_3 adopts an orientation such that the carboxyl group of Asp114 is close to the edge of the ring, so optimizing weak ionic interactions between the electronegative oxygen and the C-H dipole of an aromatic ring

Table 4

Residues that constitute the enzyme pockets of endothiapepsin

	P_6 Boc	P_5 His	P_4 Pro	P_3 Phe	P_2 His	P_1 Leu	$P_{1'}$ Val	$P_{2'}$ Ile	$P_{3'}$ His
	Leu10	Leu10	Asp12	Ile7	Tyr75	Asp30	Gly34	Ser74	
	Phe275	Asp12	Thr219	Asp12	Gly76	Asp32	Tyr75	Ser35	Tyr75
	Gly276	W4	Leu220	Ala13	Asp77	Tyr75	Gly76	Ile73	Ile299
	Pro277	W5	Tyr222	Asp114	Gly217	Asp77	Ile213	Ser74	W2
	Ile278	W176	W1	Ile117	Thr218	Ser79	Asp215	Tyr75	W197
	Phe284	W222	W3	Gly217	Ile297	Phe111	Gly217	Leu128	W206
	W5	W239	W4	Thr218	Ile301	Leu120	Thr218	Thr130	
	W176		W209	Thr219	W3	Asp215		Phe189	
	W181			W1		Gly217		W2	
				W3		Thr218		W10	
				W7		W3		W247	
				W8		W7			
						W174			
Quality of the electron density	Good	Good	Good	Good	Good	Good	Good	Good	Weak
No. of contacts	22	40	17	50	34	43	19	22	11
No. of hydrogen bonds	0	3	2	3	3	5	1	1	2
No. of hydrogen bonds to water molecules	0	1	2	1	1	0	0	0	1
C atoms of the inhibitor	4	6	5	9	6	6	6	6	3
O, N atoms of the inhibitor	2	4	2	2	4	2	1	1	2
C atoms of the enzyme	8	4	3	13	10	11	8	8	2
O, N atoms of the enzyme	3	2	2	6	6	10	4	3	2
No. of water molecules	3	5	4	4	1	3	0	3	3
Total atoms in each pocket	20	21	16	34	27	42	19	21	12
Atoms of inhibitor : enzyme	6 : 11	10 : 6	7 : 5	11 : 19	10 : 16	8 : 21	7 : 12	7 : 11	5 : 4
Accessibility in solution (Å^2)	55	54	41	56	49	51	31	55	70
Accessibility in complex (Å^2)	10	40	18	7	9	0	1	7	52

Residues that constitute the binding pockets of endothiapepsin were defined according to the distance (cut-off of 4·2 Å) and accessible contact area. The quality of the final electron density map and other relevant details of these pockets are listed. Solvent accessible areas were calculated by the method described by Richmond & Richards (1978), using a solvent probe radius of 1·4 Å. The assumption is made that the average inhibitor conformation in solution is the same as that of the complex.

(Thomas *et al.*, 1982). Phenylalanine is incorporated in most renin inhibitors, including H-261, at P_3. In most of the inhibitor complexes we have analysed, P_3 Phe takes up the same orientation with respect to Asp114. In CP69,799 (Šali *et al.*, 1989) the Phe is rotated about the C^{β}–C^{γ} bond to minimize interactions with a cyclohexyl group at P_1 and Asp114 is moved to maintain the favourable interaction.

The aspartate residues 12, 30 and 114 of endothiapepsin are replaced by Thr, Ala and Val in human renin (Sibanda *et al.*, 1984; Sielecki *et al.*, 1989). These changes, together with an additional substitution of Phe in place of Ile117, may make this sub-site larger but less polar. The extensive nature of the interactions at this sub-site is consistent with the observation that replacing Phe at P_3 by Ala reduced the potency of inhibitors for renin by 4000-fold (Boger, 1985).

(v) *Sub-site S_2*

This is a large amphiphilic sub-site that can accommodate the side-chain of P_2 in several different conformations. In the H-261 complex reported here, Gly76, Gly217, Thr218, Ile297, Ile301, Tyr75 and Asp77 make contacts to this residue. The imidazole side-chain of P_2 His is oriented towards the S'_1 subsite, which is contiguous with S_2. In other inhibitors the side-chain is often oriented towards P_4, and in the CP69,799 complex the side-chain takes up both positions with almost equal occupancy (Šali *et al.*, 1989). If both orientations of the histidyl side-chain are considered, Tyr222 should be considered part of this sub-site. There are identical residues in human renin and endothiapepsin at positions 75 and 217, but smaller side-chains at positions 77, 218, 222, 297 and 301 in human renin thereby providing a larger binding pocket.

(vi) *Sub-site S_1*

S_1 is continuous with S_3 so that the side-chain of P_1 Leu is in contact with that of P_3 Phe. This sub-site is formed by the side-chains of Tyr75, Phe111, Asp77, Asp30, Thr218 and Leu120. It is probable that Asp30 is protonated in the complex, since it is buried in a largely non-polar environment.

This pocket can accommodate side-chains larger than leucine, for example Phe in H-256 (Cooper *et al.*, 1988) and cyclohexyl in CP69,799 (Šali *et al.*, 1989; Cooper *et al.*, 1989). For human renin, homology modelling and X-ray analysis indicate that this sub-site may be slightly larger and somewhat different in shape (Sibanda *et al.*, 1984; Sielecki *et al.*, 1989). This may account for the fact that cyclo-

Table 5
Changes in solvent accessible contact area of residues due to the binding of the inhibitor

Residue	Free enzyme (Å)	Complex (Å)	Difference (Å)
Ile7	11·6	8·7	2·9
Leu10	19·9	9·2	10·8
Asp12	11·3	0·1	11·2
Ala13	4·8	0·8	4·1
Asp30	3·5	0·5	3·0
Asp32	2·2	0·0	2·2
Gly34	4·2	0·0	4·2
Ser35	2·5	0·0	2·5
Ile73	5·6	1·9	3·7
Ser74	23·1	18·9	4·2
Tyr75	13·0	2·5	10·5
Gly76	27·3	11·8	15·5
Asp77	32·6	19·1	13·4
Phe111	6·2	1·2	5·0
Asp114	12·6	7·4	5·1
Ile117	3·3	0·2	3·1
Leu120	3·7	0·0	3·6
Leu128	17·9	11·4	6·5
Thr130	11·9	9·2	2·7
Phe189	12·5	4·6	8·0
Asp215	2·3	0·0	2·3
Gly217	8·5	0·7	7·9
Thr218	10·8	0·0	10·8
Thr219	11·5	0·2	11·4
Leu220	4·3	0·4	3·9
Tyr222	13·4	8·3	5·1
Phe275	6·8	1·7	5·1
Pro277	19·4	16·8	2·6
Ile278	22·7	17·7	5·0
Phe284	13·5	4·8	8·7
Ile297	21·6	13·7	7·9
Ile299	18·3	15·1	3·1
Ile301	4·3	0·0	4·3

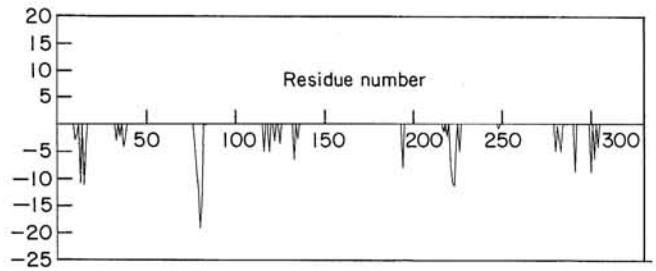

Figure 11. Differences between the solvent accessible contact areas for residues of endothiapepsin with and without the inhibitor.

(ix) *Sub-site* S'_3

P'_3 His curls out into the solvent region interacting with several water molecules. This probably accounts for the more diffuse electron density of the histidine side-chain. Thus, sub-site residues defined by interaction with this inhibitor at P'_3 cannot contribute very much to the binding. It has been suggested that potent inhibitors like H-261 may interact in a different fashion at S'_3 of human renin so accounting for the specificity observed for P'_3 histidine in substrates (Sibanda *et al.*, 1984).

(f) *Evidence for decrease in disorder and conformational change on ligand binding*

Figure 12 shows the mean isotropic temperature factors, B_{iso}, for the main-chain of the free enzyme and the complex together with their differences, plotted against residue number. Although there may be systematic differences between the *B*-values of the enzyme and its complex due to different

hexylalanine side-chains at P_1 improve the inhibition constant for human renin significantly more than leucyl or phenyl side-chains (Boger *et al.*, 1985).

(vii) *Sub-site* S'_1

The S'_1 sub-site is related to the S_1 sub-site by the inter-lobe pseudo-2-fold axis (Blundell *et al.*, 1990), and consequently resembles it in general disposition. It involves residues such as Ile213 of the C-terminal domain as well as residues of the flap including Tyr75 and Gly76. The sub-site is continuous with S_2 and larger side-chains are known to be accommodated by interactions with Ile299 and Ile301 (e.g. see Cooper *et al.*, 1987).

(viii) *Sub-site* S'_2

The S'_2 sub-site is formed by residues Ile73, Ser74, Tyr75, Leu128, Thr130 and Phe189. Water molecules are also present in spite of the hydrophobic side-chain of P'_2 Ile. This sub-site is shallow, but the isoleucine fills it well and makes multiple contacts with the enzyme (Table 4). Here the aromatic rings of Phe189 and Tyr75 are disposed on either side of the inhibitor main-chain.

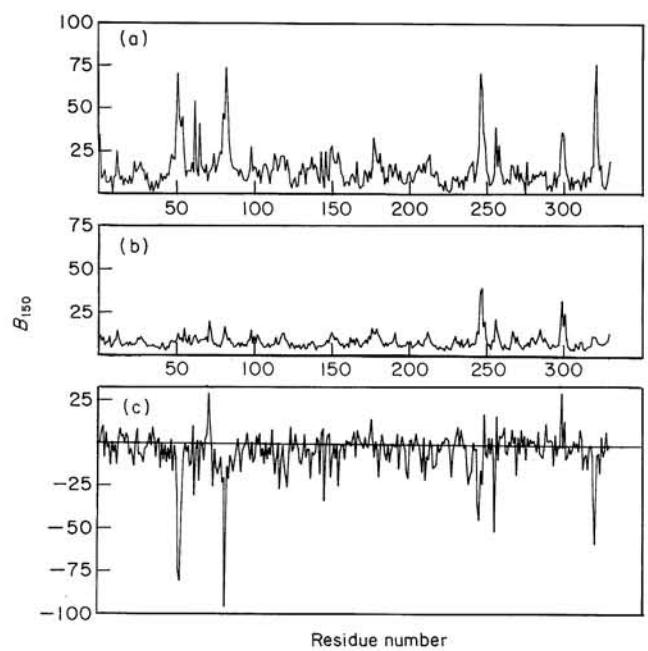

Figure 12. The main-chain *B*-values of (a) the free enzyme, (b) the enzyme–inhibitor complex and (c) the difference between bound and free forms.

Table 6
Residues that move due to inhibitor binding

Pocket	Enzyme side-chains
P_6	Phe275 (2·5 Å), Ile278 (1·2 Å)
P_5	—
P_4	—
P_3	Asp114 (3·8 Å),Glu113 (3·8 Å), Ser110 (1·7 Å)
P_2	Ile297 (3·0 Å)
P_1	Asp77 (2·3 Å), Ser79 (1·7 Å)
$P_{1'}$	—
$P_{2'}$	Thr130 (1·8 Å)
$P_{3'}$	Ser74 (1·1 Å), Ile299 (2·8 Å)

The positions of equivalent side-chains of endothiapepsin with and without inhibitor were compared. The values within parentheses are the averaged values of the distances the residues have moved. The residues whose electron density were found to be disordered in the native structure are not taken into account.

resolutions, there are several areas where differences occur which may be due to the different crystal packing. These include (1) the loop comprised of residues 48 to 59; (2) the helix comprised of residues 108 to 114 and turn residues 115 to 117; (3) the loops 234 to 237 and 240 to 243 that follow helix 225 to 233; (4) the loop of residues 317 to 320. All of these surface regions are involved in inter-molecular contacts as shown in Table 3, and thus the decrease in the thermal factors in the complex may be a consequence of the different packing in the H-261 crystals.

There are several other regions where large decreases in thermal parameters occur. Most significant of these is the flap, 71 to 82, for which there is a decrease from 30 Å^2 in the free enzyme to 8 Å^2 in the complex for main-chain atoms only.

Table 6 demonstrates that on complexation there is also a movement of residues of the flap (residues 73 to 79). The average C^α difference is about 1·0 Å, with a maximum of about 1·3 Å in the region of residues 77 to 79. However, there is a mean movement of only 0·6 Å in the Tyr75 side-chain, which is the smallest movement in the loop. The decrease in isotropic temperature factor or "mobility" and the change in position of the flap are almost certainly a consequence of the interactions described above between the inhibitor and the enzyme. These differences in the position of the flap are smaller than those reported for penicillopepsin in its complex with an inhibitor (James *et al.*, 1982). However, endothiapepsin, unlike penicillopepsin, has no intermolecular intercations involving the flap (residues 75 to 79), either in the free enzyme or in the complex. Thus, these results should be relatively unbiased by the specific crystal environment.

The significant decrease in temperature factors of helix 108 to 114 may also have contributions from inhibitor binding (Šali *et al.*, 1989) due to interactions between this helix and P_3 of H-261 (Table 4). The mean B_{iso} value of 34 Å^2 in the free enzyme is reduced to 14 Å^2 in the complex. The carboxylate groups of Glu113 and Asp114 move by about 3·8 Å and 2·8 Å, respectively. It appears the flap and helix move together on complexation with the inhibitor.

A comparison of C^α positions using a difference distance matrix (for a review, see Richards & Kundrot, 1988) was made between the native and complexed endothiapepsin. The comparison revealed small but significant changes in the relative orientation of two rigid bodies, the first one comprising residues −2 to 189, and 304 to 326, and the second one consisting of residues 190 to 303. For the H-261 complex the movement may be considered as a 4·2° rotation of the smaller carboxy-terminal domain and a 0·25 Å shift parallel to the rotation axis. This screw axis passes approximately through the C^α atoms of residues 22 and 213, and also through the active site aspartate residues. The effect also occurs with the H-261 complex when co-crystallized in the native-like crystal form. The relative rotation of 0·6° and the translation of 0·16 Å are in the same direction as those crystals reported here, but they are much smaller. We shall discuss the rigid body rotation in 20 inhibitor complexes of endothiapepsin in a separate publication (A. Šali *et al.*, unpublished results). Clearly crystal packing plays a role but it is not the only factor.

(g) *Factors affecting binding affinity*

The solvent contact area of the free enzyme, calculated by the method described by Richmond & Richards (1978), decreases by 200 Å^2 on inhibitor binding; this corresponds to about 5% of the total surface area. The inhibitor loses about 313 Å^2 of its surface area, which corresponds to 68% of its total surface area, assuming that the average solution conformation is the same as the bound one.

The central region of the inhibitor (-Leu-CHOH-CH_2-Val-) is completely excluded from the solvent. Residues P_6, P_3, P_2 and P'_2 also become largely inaccessible on binding to the enzyme (Table 4). The hydrophilicity of the pockets gradually increases on either side of the catalytic centre. Pockets S_2, S_1, S'_1 and S'_2 are relatively hydrophobic, whereas pockets S_4, S_3 and S'_3 are more hydrophilic. This is reflected in the ratio of contacts involving carbon to those involving nitrogen and oxygen atoms in the sub-sites (Table 4).

The free energy due to the hydrophobic effect plays an important part in the tight binding of the inhibitor. If it is assumed that burying 1 Å^2 of the amino acid surface contributes approximately −0·4 kJ/mol to the free energy of the reaction (Chothia, 1974; Richmond & Richards, 1978), the contribution of the hydrophobic effect of inhibitor binding to the enzyme is −207 kJ/mol, but the experimentally determined total standard free energy of binding at 25 °C is about −51 kJ/mol. The difference between these two values includes contributions from the loss of entropy of the inhibitor, flap and many side-chains of the enzyme.

Comparison of the hydrogen bonds of various oligopeptide inhibitors reveals that there is an absolute conservation of the mode of binding of the main-chain of the inhibitor to the enzyme. Also, water molecules that are hydrogen-bonded in the active site cleft in the native enzyme are displaced on complexation and are replaced by hydrogen bonding donors or acceptors of the inhibitor. This replacement leads to a small free energy contribution of hydrogen bonding to the ligand binding (Fersht *et al.*, 1986). This suggests that the crucial role played by the conserved main-chain hydrogen bonds of the ligand is a precise alignment of the substrate with the catalytic residues of the enzyme (Šali *et al.*, 1989).

We thank the SERC Molecular Recognition Initiative for financial support, and the MRC for a studentship to J.B.C. A.S. was funded by the Research Council of Slovenia, the J. Stefan Institute and Merck Sharpe and Dohme. We are grateful to Professor Michael Szelke and colleagues for providing the inhibitor, and to Drs Ian Tickle, Stephen Foundling and Stephen Wood for much help and advice.

References

Berger, A. & Schechter, I. (1970). *Phil. Trans. Roy. Soc. ser. B*, **257**, 249–254.

Blundell, T. L., Jenkins, J., Peearl, L. & Sewell, B. T. (1985) In *Aspartic Proteinases and their Inhibitors* (Kostka, V., ed.), pp. 151–161, de Gruyter, Berlin.

Blundell, T. L., Cooper, J., Foundling, S. I., Jones, D. M., Atrash, B. & Szelke, M. (1987). *Biochemistry*, **26**, 5585–5590.

Blundell, T. L., Jenkins, J. A., Sewell, B. T., Pearl, L. H., Cooper, J. B., Tickle, I. J., Veerapandian, B. & Wood, S. P. (1990). *J. Mol. Biol.* **211**, 919–941.

Boger, J. (1985) In *Aspartic Proteinases and their Inhibitors* (Kostka, V., ed.), pp. 401–420, de Gruyter, Berlin.

Boger, J., Payne, L. S., Perlow, D. S., Lohr, N. S., Poe, M., Blaine, E. H., Ulm, E. H., Schorn, T. W., LaMont, B. I., Lin, T. Y., Kawai, M., Rich, D. H. & Veber, D. (1985). *J. Med. Chem.* **28**, 1779–1790.

Bott, R., Subramanian, E. & Davies, D. (1982). *Biochemistry*, **21**, 6956–6962.

Chothia, C. (1974). *Nature (London)*, **248**, 338–339.

Cooper, J. B. (1989). Ph.D. thesis, University of London.

Cooper, J. B. & Harris, C. J. (1989). *Curr. Cardiovasc. Patents*, **1**, 143–157.

Cooper, J., Foundling, S., Hemmings, A., Blundell, T. L., Jones, D. M., Hallett, A. & Szelke, M. (1987). *Eur. J. Biochem.* **169**, 215–221.

Cooper, J. B., Foundling, S. I., Blundell, T. L., Arrowsmith, R. J., Harris, C. J. & Champress, J. M. (1988). In *Topics in Medicinal Chemistry* (Leeming, P. R., ed.), Roy. Soc. Chem. Special Publication 65, pp. 308–313, London.

Cooper, J. B., Foundling, S. I., Blundell, T. L., Boger, J., Jupp, R. & Kay, J. (1989). *Biochemistry*, **28**, 8596–8603.

Cooper, J. B., Khan, G., Taylor, G., Tickle, I. J. & Blundell, T. L. (1990). *J. Mol. Biol.* **214**, 199–222.

Fersht, A. R., Leatherbarrow, J. R. & Wells, T. N. C. (1986). *Phil. Trans. Roy. Soc. ser A*, **317**, 305–320.

Foundling, S. I., Cooper, J. B., Watson, F. E., Cleasby, A., Pearl, L. H., Sibanda, B. L., Hemmings, A., Wood, S. P., Blundell, T. L., Valler, T. L., Norey, C. G., Kay, J., Boger, J. Dunn, B. M., Leckie, B. J., Jones, D. M., Atrash, B., Hallett, A. & Szelke, M. (1987). *Nature (London)*, **327**, 349–352.

Haneef, I., Moss, D. S., Stanford, M. J. & Borkakoti, N. (1985). *Acta Crystallogr. sect. A*, **41**, 426–433.

James, M. N. G. & Sielecki, A. (1985). *Biochemistry*, **24**, 3701–3713.

James, M. N. G., Sielecki, A. R., Salituro, F., Rich, D. H. & Hofmann, T. (1982). *Proc. Nat. Acad. Sci., U.S.A.* **79**, 6137–6142.

Janin, J., Wodak, S., Levitt, M. & Maigret, B. (1978). *J. Mol. Biol.* **125**, 357–386.

Jones, T. A. (1978). *J. Appl. Crystallogr.* **11**, 268–272.

Luzzati, V. (1952). *Acta Crystallogr.* **5**, 802–810.

McLachlan, A. D. (1982). *Acta Crystallogr. sect. A*, **38**, 871–873.

Moews, P. & Bunn, C. W. (1970). *J. Mol. Biol.* **54**, 395–397.

Moss, D. S. & Morffew, A. J. (1982). *Comput. Chem.* **6**, 1–3.

North, A. C. T., Phillips, D. C. & Mathews, F. S. (1968). *Acta Crystallogr. sect. A*, **24**, 359.

Ondetti, M. A. & Cushman, D. W. (1980). *Annu. Rev. Biochem.* **51**, 283–308.

Pearl, L. H. (1985) In *Aspartic Proteinases and their Inhibitors* (Kotska, V., ed.), pp. 189–195, de Gruyter, Berlin.

Pearl, L. & Blundell, T. L. (1984). *FEBS Letters*, **174**, 96–101.

Rae, A. D. (1965). *Acta Crystallogr.* **19**, 683–684.

Rae, A. D. & Blake, C. (1966). *Acta Crystallogr.* **20**, 586.

Rich, D. H. & Bernatowicz, M. S. (1982). *J. Med. Chem.* **25**, 791–795.

Rich, D. H., Sun, E. T. O. & Ulm, E. (1980). *J. Med. Chem.* **23**, 27–33.

Richards, A. D., Roberts, R. F., Dunn, B. M., Graves, M. C. & Kay, J. (1989). *FEBS Letters*, **247**, 113–117.

Richards, F. M. & Kundrot, C. E. (1988). *Proteins*, **3**, 71–84.

Richmond, T. J. & Richards, F. M. (1978). *J. Mol. Biol.* **119**, 537–555.

Šali, A., Veerapandian, B., Cooper, J. B., Foundling, S. I., Hoover, D. J. & Blundell, T. L. (1989). *EMBO J.* **8**, 2179–2188.

Sibanda, B. L., Blundell, T. L., Hobart, P. M., Fogliano, M., Bindra, J. S., Dominey, B. W. & Chirgwin, J. M. (1984). *FEBS Letters*, **174**, 102–111.

Sielecki, A. R., Hayakawa, K., Fujinaga, M., Fraser, M., Muir, A. K., Carilli, C. T., Lewicki, J. A., Baxter, J. D. & James, M. N. G. (1989). *Science*, **243**, 1346–1351.

Singh, T. P., Haridas, M., Chauhan, V. S. & Kumar, A. (1987). *Biopolymers*, **26**, 819–829.

Suguna, K., Padlan, E. A., Smith, C. W., Carlson, W. D. & Davies, D. (1987). *Proc. Nat. Acad. Sci., U.S.A.* **84**, 7009–7013.

Szelke, M., Leckie, B. J., Hallett, A., Jones, D. M., Suerias-Diaz, J., Atrash, B. & Lever, A. F. (1982). *Nature (London)*, **299**, 555–557.

Szelke, M., Tree, M., Leckie, B. J., Jones, D. M., Atrash, B., Neattie, S., Donovan, B., Hallett, A., Hughes, M., Lever, A. F., Morton, J. J. & Sueiras-Diaz, J. (1985). *J. Hyperten.* **3**, 13–18.

Thomas, K. A., Smith, G. A., Thomas, T. B. & Feldman, R. S. (1982). *Proc. Nat. Acad. Sci., U.S.A.* **79**, 4843–4847.

Tickle, I. J. (1988). In *Improving Protein Phases* (Bailey, S., Dodson, E. & Phillips, S., eds), pp. 130–137, SERC, Daresbury Laboratory.

Tree, M., Donovan, B., Gamble, J., Hallet, A., Hughes, M., Jones, D. M., Leckie, B., Lever, A. F., Morton, J. J. & Szelke, M. (1983). *J. Hyperten.* **1**, 399–403.

Umezawa, H., Aoyagi, T., Morishima, H., Matzusaku, M., Hamada, H. & Takeuchi, T. (1970). *J. Antibiot.* **23**, 259–262.

Webb, D. J., Manhem, J. O. P., Ball, S. G., Inglis, G., Leckie, B. J., Lever, A. F., Morton, J. J., Robertson, J. I. S., Murray, G. D., Menard, J., Hallett, A., Jones, D. M. & Szelke, M. (1985). *J. Hyperten.* **3**, 653–658.

Whitaker, J. R. (1970). *Methods Enzymol.* **19**, 436–445.

Workman, R. J. & Burkitt, D. W. (1979). *Arch. Biochem. Biophys.* **194**, 157–164.

Edited by R. Huber